



HAL
open science

Effect of temperature and initial state on variation of thermal parameters of fine compacted soils

Ahmed Boukelia, S. Rosin-Paumier, Hossein Eslami, Farimah Masrouri

► **To cite this version:**

Ahmed Boukelia, S. Rosin-Paumier, Hossein Eslami, Farimah Masrouri. Effect of temperature and initial state on variation of thermal parameters of fine compacted soils. *European Journal of Environmental and Civil Engineering*, 2017, 23 (9), pp.1125-1138. <10.1080/19648189.2017.1344144>. <hal-01717778>

HAL Id: hal-01717778

<https://hal.science/hal-01717778v1>

Submitted on 18 Jun 2018

HAL is a multi-disciplinary open access archive for the deposit and dissemination of scientific research documents, whether they are published or not. The documents may come from teaching and research institutions in France or abroad, or from public or private research centers.

L'archive ouverte pluridisciplinaire **HAL**, est destinée au dépôt et à la diffusion de documents scientifiques de niveau recherche, publiés ou non, émanant des établissements d'enseignement et de recherche français ou étrangers, des laboratoires publics ou privés.



HAL Authorization

18 **1. Introduction**

19 Soil thermal properties are required in some engineering applications such as the design of
20 high-level radioactive waste disposals (Rutqvist, Wu, Tsang, & Bodvarsson, 2002), buried
21 power transmission (De Lieto Vollaro, Fontana, & Vallati, 2011), energy geostructures
22 (Pahud, 2002 and Brandl, 2006) and thermal energy storage (Navarro et al., 2016 and
23 Giordano, Comina, Mandrone, & Cagni, 2016). The study of heat flow in soil is based on the
24 thermal properties and temperature gradient. The thermal parameters governing the transfer of
25 heat are the **thermal conductivity** (λ), which is the ability of the material to conduct heat, the
26 **volumetric heat capacity** (C), which describes the ability of the material to store thermal
27 energy while undergoing a given temperature change, and the **thermal diffusivity** ($\alpha = \lambda/C$),
28 which describes the ability of a material to conduct thermal energy relative to its ability to
29 store thermal energy.

30 A variety of measurement techniques are available for natural materials with a broad
31 temperature range. Recently, Zhang, Cai, Liu & Puppala (2016) presented most commonly
32 used measurement techniques such as the steady-state method, the transient hot-wire method,
33 the laser flash diffusivity method and the transient plane source method. The hot-wire method
34 also known as the needle-probe method (ASTM, 2000) is a transient technique that measures
35 temperature rise at a known distance from a linear heat source embedded in the test sample.
36 This method is widely used in natural soil and compacted soil characterization for its
37 accuracy, speed and simple application.

38 The thermal parameters (λ , C and α) depend on soil parameters such as the mineralogy, water
39 content, bulk density, particle size distribution and structural arrangement (Abu-Hamdeh
40 (2001), Abu-Hamdeh (2003), Tang (2005), Brandl (2006), Ehdezi (2012)). Abu-Hamdeh and
41 Reeder (2000) measured the thermal conductivity of four soils as a function of their water
42 content and density. The authors noted that for each soil, λ increased with increasing density.

43 Similarly, when the water content increased λ , increased as well. The results of Tang (2005)
44 showed the same trends for a clayey material. Barry-Macaulay, Bouazza, Singh, Wang, and
45 Ranjith (2013) presented the same type of results as part of their important database of
46 Australian natural materials. For instance, as the thermal conductivity of solid particles
47 exceeds those of the air and the water, an increase in the dry density results in an increase in
48 λ . Furthermore, increasing the contact surface between solid particles increases the heat flux
49 and results in an increase of λ . In the same way, as the thermal conductivity of water is higher
50 than that of the air, an increase in the saturation rate results in an increase in λ .

51 Few studies have been conducted on the thermal conductivity of compacted soils. Ekwue,
52 Stone, and Bhagwat (2006) studied the combined effects of soil density and water content on
53 soil thermal conductivity of three soils: a sandy loam, a clayey loam and a clay. They
54 measured the thermal conductivity for different values of water content and dry density on the
55 compaction curve of these soils. For each soil, λ reaches a maximal value near the Proctor
56 optimum water content. The study of Ekwue et al. (2006) was also focused on the impact of
57 soil mineralogy on λ , and the material with a high sand content showed the most important
58 impact. However, the coupled effect of soil density and water content on the volumetric heat
59 capacity and thermal diffusivity was not well studied. The monotonic and cyclic heat effect on
60 thermal parameters was also not studied.

61 Several prediction models of soil thermal parameters, taking into account the soil properties,
62 are available to evaluate the thermal conductivity (De Vries (1963), Johansen (1977) and
63 Kersten (1949)). For example, Farouki (1981) and, more recently, Dong, John, McCartney,
64 and Lu (2015) presented an extensive review of the numerous available prediction models.
65 However, these models are perfectible (Dong et al. 2015) and need to be improved to take
66 into account new environmental or industrial issues such as soil temperature.

67 In civil engineering, the temperature variation range evolves according to the process; for
68 example, cyclic variations from 4 and 30°C were recorded for heat exchange piles (Peron,
69 Knellwolf, & Laloui, 2011) a maximum temperature of 70°C was estimated for thermal
70 energy storage (Giordano et al. 2016), 100°C was used for the design of high-level radioactive
71 waste disposal (Tang, 2005), and 90°C was used in the design of buried power transmission
72 cables (Hanna, Chikhani, & Salama, 1993). Temperature variations affect the physical
73 properties of soil (solid and water particles volumetric variation and change in water status),
74 inducing changes in the thermal properties. Considering the impact of temperature on the
75 thermal proprieties of soils between 0° and 70°C, only a few studies are available. Hiraiwa
76 and Kasubuchi (2000) measured the thermal conductivity of two soils, a clay loam and a light
77 clay, at different volumetric water contents and different temperatures between 5 and 75°C.
78 Their results showed that λ increased with increasing temperature and volumetric water
79 content. Smits, Sakaki, Howington, Peters, and Illangasekare (2013) measured the thermal
80 conductivity and diffusivity of two sands prepared at various saturation rates at different
81 temperatures between 30 and 70°C. Their results showed that the thermal properties increased
82 dramatically for temperatures above 50°C, but small changes in thermal properties were
83 observed at temperatures between 30 and 50°C.

84 This literature review shows that numerous studies are available on the impact of soil
85 parameters on the soil thermal conductivity; some of these studies address compacted soils,
86 but fewer focus on the compacted soils used in civil engineering that are submitted to cyclic
87 temperature variations from 1 to 70°C. Furthermore, few studies and little data are available
88 on the variation of the volumetric heat capacity and the thermal diffusivity as a function of
89 soil properties, despite their great importance in the study of heat flow and heat storage in
90 soils.

91 The aim of this study was to better understand the coupled effect of water content (w),
92 dry density (ρ_d) and temperature variations (T) on the thermal parameters (λ , C and α) of
93 compacted soils. The following issues were addressed:

- 94 • whether the mineralogy and the size distribution of soil particles affect their thermal
95 properties,
- 96 • the coupled effect of w and ρ_d on the thermal parameters, and
- 97 • the effect of monotonic and cyclic thermal variation on soil thermal characteristics.

98 In the following sections, the preparation of the materials and the experimental device are
99 described first. Then, the results are presented and analysed to explain the main evolutions of
100 the thermal properties according to the initial state parameters of compacted soils and the
101 impact of thermal variations.

102 **2. Materials and methods**

103 In this section, the properties of the five studied materials, the compaction of the materials at
104 various water contents and dry densities, and the apparatus used to measure the thermal
105 properties are presented.

106 **2.1. The materials properties**

107 Five different soils were studied. The mineralogical compositions of these soils are presented
108 in *Table 1*. The illitic soil (I) named Arginotech® came from eastern Germany. The Plaisir
109 loam (PL) was extracted from the Paris region and was dried, pulverized and sieved through a
110 2 mm sieve before being quartered and used for various experiments (Boukelia, 2016). Two
111 other loams from the Parisian basin, namely, the Jossigny loam (JL) and the Xeuilley loam
112 (XL), were also studied. The characteristics of each material including grain size distribution,
113 Atterberg limits (AFNOR, 1993), specific surface (AFNOR, 1999a), carbonate content
114 (AFNOR, 1996) and Proctor compaction parameters (AFNOR, 1999b) are listed in *Table 2*.

115 The particle size distributions were determined using a Laser diffraction particle size analyser
116 (Malvern Mastersizer 2000®) (AFNOR, 2009) for the illitic material (Eslami, Rosin-Paumier,
117 Abdallah, & Masrouri, 2015) and a wetting sieve method for the Plaisir loam. For the
118 Jossigny and Xeuilley loams, the particle size distribution curves were found in the literature
119 (Fleureau & Inderto, 1993 and Blanck, Cuisinier, & Masrouri, 2011). The Proctor optimum
120 water contents (w_{OPN}) and maximum dry densities (ρ_{dmax}) were obtained from the standard
121 Proctor curve performed for each mixture (AFNOR, 1999b) (*Figure 1* and *Table 3*).

122 **2.2. Sample preparation**

123 Six test series were performed (*Table 5*). In the first series, the effect of the dry density was
124 studied on an illitic soil (I) and a sand-illitic mixture (S+I). In the second series, the effect of
125 water content was studied on the same soils (I and S+I). In the third series, the effect of
126 particle size and mineralogy were evaluated for each soil. Then, the coupled effect of dry
127 density and water content was analysed by measuring the thermal properties of five materials
128 compacted at various water contents and dry densities using constant compaction energy (4th
129 series). Then, the temperature effect was studied on PL, I and S+I by measuring the thermal
130 properties of different points on a compaction curve at varying temperatures within the range
131 of 1 to 70°C (5th series). Finally, the effect of cyclic temperature variations was studied on PL
132 (6th series).

133 To prepare samples at the desired water content and dry density, powdered material was first
134 mixed with water to reach the target water content and then packed into hermitic bags to
135 homogenize over at least 24 h. Two types of samples were prepared. For the 1st and 2nd series,
136 samples 70 mm in height and 35 mm in diameter were statically compacted. For the 3rd
137 through 6th series, samples 116 mm in height and 152 mm in diameter were dynamically
138 compacted in three layers in a CBR (Californian Bearing Ratio) mould. The standard Proctor

139 compaction energy was applied. The samples were then heated or cooled to different
140 temperatures in a climatic chamber, and the thermal properties of each sample were measured.

141 **2.3. Thermal parameter measurements**

142 The thermal properties were measured using a *KD2 Pro* thermal properties analyser®. Two
143 specific sensors were used: a dual-needle SH-1 and a single needle TR-1. The dual-probe SH-
144 1 consists of two parallel probes (30 mm long and 1.3 mm diameter with 6 mm spacing). One
145 of these probes comprises a thermistor, and the other comprises the heater element. This
146 sensor measures thermal conductivity (λ), thermal resistivity (R), thermal diffusivity (α) and
147 volumetric heat capacity (C) by employing the dual needle heat pulse method. The single
148 needle TR-1 (2.4 mm diameter and 100 mm long) measures only thermal conductivity (λ);
149 this is used when λ is higher than $2 \text{ W.m}^{-1}.\text{K}^{-1}$. The measurement range and the precision of
150 both sensors are summarized in *Table 5*.

151 To measure the thermal parameters of sample, the probe was covered by a thin layer of grease
152 (Arctiv Silver® 5 – High-density polysynthetic silver thermal compound) and then was
153 placed in the sample after soil drilling at the same diameter. In this case, the use of the grease
154 is recommended to improve the contact between the sensor needle and the soil. A waiting
155 time of 15 minutes was imposed before each test to reach an equilibrium temperature between
156 the probe and the soil. The presented value is a mean value of 4 tests in different locations of
157 the sample.

158 **3. Experimental results and discussion**

159 In the following sections, the experimental results and discussions for each series are
160 presented successively.

161 **3.1. Dry density effect on thermal parameters (1st series)**

162 The effects of dry density on thermal parameters are studied on both illitic material (I) and a
163 sand-illitic mixture (S+I). Illitic samples were prepared at an initial water content in the range
164 of 28.8 to 33.4% and dry densities varying from 1.20 to 1.52 Mg/m³. Sand-illitic (S+I)
165 samples were prepared at an initial water content (*w*) in the range of 16.9 to 20.4% and dry
166 densities (ρ_d) varying from 1.54 to 1.79 Mg/m³. The variations of water content and dry
167 density were chosen in the same range of the standard Proctor curve for both materials. The
168 samples were thus prepared at water contents and dry densities compatible with their use in
169 geotechnical engineering. The real density (ρ_h) of the samples can be determined from Eq. 1.

170
$$\rho_h = (1 + w) \times \rho_d$$

(Eq. 1)

171 The results (*Figure 2a, b, c*) showed that the thermal conductivity, volumetric heat capacity
172 and thermal diffusivity increased with increasing dry density for both materials regardless of
173 the water content. Linear increases in λ , *C* and α as functions of increasing dry density were
174 shown, in agreement with literature.

175 The thermal diffusivities ($\alpha=\lambda/C$) measured on the illitic samples were significantly lower
176 than those of the sand-illitic samples.

177 **3.2. Water content effect on thermal properties (2nd series)**

178 The effect of water content on the thermal proprieties was showed by Tang (2005), Brandl
179 (2006) and Barry-Macaulay et al. (2013). In *Figure 2*, the range variations of water content
180 and dry density of I and S+I samples were the same as those in part 3.1. The enhancement of
181 thermal conductivity as a function of water content increase was clearly observed (*Figure 2a*).
182 *Figure 2b* showed that the volumetric heat capacity of both materials varied in the same
183 range. The range variation of *w* has a negligible impact on the thermal diffusivity of both

184 materials. The results obtained in the 1st and 2nd series are in agreement with literature. They
185 therefore validated the experimental procedure used in this study.

186 **3.3. Mineralogy and particle size effect on thermal properties (3rd series)**

187 The mineralogy of the sample has an effect on its thermal conductivity (Ekwue et al. 2006,
188 Zhang et al., 2017). For example, Brigaud and Vasseur (1989) denoted that the λ of quartz
189 ($\lambda_{\text{quartz}} = 7.7 \text{ W.m}^{-1}.\text{K}^{-1}$) is higher than that of illite ($\lambda_{\text{illite}} = 1.85 \text{ W.m}^{-1}.\text{K}^{-1}$). As a
190 consequence, the addition of sand to illitic material provided a higher λ for the S+I samples in
191 comparison with the illitic samples (*Figure 2a*).

192 **3.4. Coupled effect of water content and dry densities on thermal properties** 193 **(4th series)**

194 The coupled effect of water content and dry density was studied by measuring the thermal
195 parameters of samples compacted on several points of the compaction curves of five materials
196 (illite (I), illite+sand (S+I), Plaisir loam (PL), sand+Jossigny loam (S+JL), sand+Xeuilley
197 loam (S+XL)) of varying size distribution and mineralogy. Measurements of thermal
198 parameters (λ , C and α) were carried out on samples prepared with the same compaction
199 energy.

200 The results (*Figure 3*) showed that the thermal conductivity of each material increased on the
201 dry side of the compaction curve until reaching a maximum near the Proctor optimum. On the
202 dry side of the compaction curve, the dry density and the water content both increased,
203 resulting in an increase of λ . In contrast, on the wet side of the compaction curve, the
204 evolutions are different according to the sample mineralogy. For the silicious materials (S+I,
205 PL, S+JL, S+XL), λ decreased, whereas for the silicate material (I), λ remained at its highest
206 values. These evolutions are consistent with the physical properties of the studied samples. On
207 the wet side of the compaction curve, the water content continues to increase, whereas the dry

208 density decreases. As the saturation rate remains approximately the same, the water molecules
209 took the place of solid grains. As λ_{quartz} ($7.7 \text{ W.m}^{-1}.\text{K}^{-1}$) is higher than λ_{water} ($0.61 \text{ W.m}^{-1}.\text{K}^{-1}$)
210 (Brigaud & Vasseur, 1989), the thermal conductivity of samples containing quartz decreased
211 quite quickly, whereas the thermal conductivity of samples containing silicates ($\lambda_{\text{illite}} = 1.9$
212 $\text{W.m}^{-1}.\text{K}^{-1}$) remained at an approximately constant value.

213 The volumetric heat capacity of soils increased on the dry side of the compaction curve until
214 reaching a maximum near the Proctor optimum. Then, the values remained constant or
215 decreased slightly. The variation range of the volumetric heat capacity was identical for the
216 five materials studied.

217 The thermal diffusivity followed the same variation as the thermal conductivity in accordance
218 with its definition ($D=\lambda/C$). Consequently, the thermal diffusivities of sand-loam mixtures
219 (S+JL and S+XL) were three times higher than that of the illitic soil.

220 **3.5. Combined effect of water content, dry density and temperature variations on** 221 **thermal properties (5th series)**

222 According to the potential use of compacted soils near a heat source or heat sink (energy
223 storage, buried cables, or waste storage), the effect of temperature on the thermal properties
224 was studied within a maximum temperature range of 1 to 70°C. Samples were prepared at
225 various w and ρ_d under the same compaction energy (standard Proctor). Three materials were
226 investigated: the illitic material (I, *Figure 4*), the sand-illitic soil mixture (S+I, *Figure 5*) and
227 the Plaisir loam (PL, *Figure 7* and *Figure 8*). Thermal diffusivity measurements for the I
228 samples were quite scattered due to their very low values compared with the measurement
229 range (*Table 4*). In the studied temperature range, the main evolutions obtained in the
230 previous part were observed for each material:

- 231 - thermal parameters reached their maximum values near the Proctor optimum;
- 232 - thermal parameters increased on the dry side of the compaction curve;

233 - thermal parameters remained at their maximal values on the wet side of the
234 compaction curve for illitic samples; and

235 - thermal parameters decreased on the wet side of the compaction curve for the S+I and
236 PL samples.

237 Following this general trend, variations were noticed according to the sample temperature. An
238 extensive experimental study was carried out on the illitic material, which was expected to be
239 the material most sensitive to temperature variation. The uncertainty of this method (10%) is
240 presented with a double arrow for one point of each series (*Figure 4a, b and c*). The variation
241 of λ in the temperature range of 1 to 40°C was within this uncertainty interval, but for 70°C
242 results have clearly shown an increase of λ with increasing temperature. Measurements
243 performed on S+I and PL over a maximal temperature range of 1–50°C confirmed this trend.
244 The increase of thermal conductivity linked to the sample temperature was more important on
245 the dry side than on the wet side of the compaction curve. This phenomenon is in addition to
246 the increase of λ linked to the dilatation of the components (water and minerals) with
247 increasing temperature.

248 In a saturated soil, the heat flux moves through solids and liquids by diffusion. Convection
249 movements may aid the transfer, but the liquid convection may be limited, especially in low
250 permeability materials. In an unsaturated soil, at low saturation rates, as is the case on the dry
251 side of the compaction curve, the material contains solids, water and air. The thermal
252 conductivity of air is very low unless it contains water vapour. The water vapour moves
253 through the pores, increasing the thermal conductivity of the material. At higher temperatures,
254 the air is able to reach higher moisture contents, which increases its participation in thermal
255 conduction.

256 The impact of temperature variations on the volumetric heat capacity was not as clear as that
257 on λ , especially for the I and S+I samples. *Figure 4b and 5b* do not show a clear trend for the

258 evolution of this parameter. The impact of temperature variations seemed to be below the
259 measurement sensitivity. For PL samples, C measurements at 50°C were higher than values at
260 20°C in the case of L1 samples (*Figure 8*). The thermal diffusivity increased with increasing
261 temperature in accordance with the λ evolution (*Figure 4c* and *5c*).

262 **3.6. Cyclic temperature variation effect on thermal properties (6th series)**

263 Several samples of Plaisir loam were submitted to cyclic variations of temperature. Different
264 cycles of 20/50°C (*Table 6*) were applied to the samples that were hermetically closed to keep
265 w constant. The measurements were performed at various steps of the temperature
266 programmes, as defined in *Figure 6*.

267 The experimental results showed that heating the samples increased the thermal conductivity
268 and the volumetric heat capacity. These results confirmed the trends obtained in the previous
269 part.

270 The measurements after 60 cycles showed that the **thermal conductivity** λ_{PL} at 20°C after the
271 thermal cycles (C3) was lower than λ_{PL} at 50°C (C2). Nevertheless, the value of λ_{PL} at 20°C
272 measured after the cycles (C3) was slightly higher than λ_{PL} at 20°C measured at the beginning
273 of the test (C1) (*Figure 7*). The thermal conductivity reflects the capacity of a material to
274 conduct a heat flux, this difference can be due to a change in the soil structure after several
275 cycles.

276 Measurements of the **volumetric heat capacity** at 20°C (C3) remained very close to those
277 obtained in test (C1) (*Figure 8*). The volumetric heat capacity reflects the ability of a material
278 to store energy, it may be considered as the sum of the participation of soil different
279 component. The ratio between solid, liquid and air did not vary in the sample and the
280 volumetric heat capacity remained unchanged.

281 **4. Conclusions**

282 The effects of dry density, water content, mineralogy, size distribution and temperature on the
283 thermal conductivity, volumetric heat capacity and thermal diffusivity of five materials were
284 studied in the laboratory. In accordance with previous studies, the thermal parameters of the
285 studied materials increased with increasing dry density and water content. The samples with
286 wider granularity had a higher density and better solid contacts that improved their thermal
287 conductivity. The effect of water content on thermal conductivity was clearly observed in
288 loose materials, whereas in denser materials, the effect was negligible. The thermal
289 conductivity of materials increased with increasing quartz percentage and the spread of the
290 granulometric curve, whereas the volumetric heat capacity of materials seemed less sensitive
291 to variations in the mineralogy and particle size. In the compacted soils, the thermal
292 conductivity, the volumetric heat capacity and the diffusivity increased on the dry side of the
293 compaction curve until reaching a maximum near the Proctor optimum.

294 The effect of temperature variation on the thermal properties was studied within a maximum
295 temperature range of 1 to 70°C. The thermal conductivity and thermal diffusivity increased
296 significantly on the dry side of the compaction curve and at high temperatures (illitic soil at
297 70°C), while the effect of temperature on the specific heat capacity was not significant. The
298 increase in thermal conductivity induced by temperature variation was more important on the
299 dry side than on the wet side of the compaction curve due to the water vapour movement.
300 Heating the samples increased the thermal properties, but this modification is partially
301 reversible after several cycles for thermal conductivity and totally reversible for volumetric
302 heat capacity.

303

304

305 **5. References:**

306 AFNOR. (1993). *NF P94-051 Sols: reconnaissance et essais; Détermination des limites*
307 *d'Atterberg-Limite de liquidité à la coupelle-Limite de plasticité au rouleau* [Soil:
308 Investigation and testing. Determination of Atterberg's limits. Liquid limit test using
309 cassagrande apparatus. Plastic limit test on rolled thread] (p. 15). Paris: Association Française
310 de Normalisation.

311 AFNOR. (1996). *NF P 94-048: Sols : Reconnaissance et Essais – Détermination de la teneur*
312 *en carbonate –Méthode du calcimètre* (p.11). Paris: Association Française de Normalisation.

313 AFNOR. (1999a). *NF EN 933-9: Tests for geometrical properties of aggregates - Part 9:*
314 *Assessment of fines-Methylene blue test* (p.12). Paris: Association Française de Normalisation.

315 AFNOR. (1999b). *NF P 94-093 Sols: Reconnaissance et essais Détermination des références*
316 *de compactage d'un matériau. Essai Proctor Normal-Essai Proctor Modifié* [Soils:
317 Investigation and testing. Determination of the compaction characteristics of a soil. Standard
318 Proctor test. Modified Proctor test] (p. 18). Paris: Association Française de Normalisation.

319 AFNOR. (2009). *ISO 13320: Particle size analysis–Laser diffraction methods* (p.60). Paris:
320 Association Française de Normalisation.

321 Abu-Hamdeh, N.H. (2001). Measurement of the Thermal Conductivity of Sandy Loam and
322 Clay Loam Soils using Single and Dual Probes. *Journal of Agricultural Engineering*
323 *Research*, 80(2), 209–216.

324 Abu-Hamdeh, N.H. (2003). Thermal Properties of Soils as affected by Density and Water
325 Content. *Biosystems Engineering*, 86(1), 97–102.

326 Abu-Hamdeh, N.H., & Reeder, R.C. (2000). Soil Thermal Conductivity: Effects of Density,
327 Moisture, Salt Concentration, and Organic Matter. *Soil Science Society of America Journal*,
328 64(4), 1285–1290.

329 Barry-Macaulay, D., Bouazza, A., Singh, R. M., Wang, B., & Ranjith, P. G. (2013). Thermal
330 conductivity of soils and rocks from the Melbourne (Australia) region. *Engineering Geology*,
331 164, 131–138.

332 Blanck, G., Cuisinier, O., & Masrouri, F. (2011, September). *Effet d'un traitement non*
333 *traditionnel acide sur le comportement mécanique de trois limons*. 20^{ème} Congrès Français de
334 Mécanique, Besançon, France.

335 Boukelia, A. (2016). *Modélisation physique et numérique des géo-structures énergétiques*.
336 (PhD thesis). Université de Lorraine, Nancy, France.

337 Brandl, H. (2006). Energy foundations and other thermo-active ground structures.
338 *Géotechnique*, 56(2), 81–122.

339 Brigaud, F., & Vasseur, G. (1989). Mineralogy, porosity and fluid control on thermal
340 conductivity of sedimentary rocks. *Geophysical Journal International*, 98, 525–542.

341 Dong, Y., McCartney, J.S. & Lu, N. (2015). Critical Review of Thermal Conductivity Models
342 for Unsaturated Soils. *Geotechnical and Geological Engineering*, 33(2), 207-221.

343 De Vries, D. A. (1963). Thermal properties of soils. *Physics of Plant Environment*. North-
344 Holland, Amsterdam.

345 Ehdezi, P.K. (2012). *Enhancing Pavements for Thermal Applications*. (PhD thesis).
346 University of Nottingham, Royaume-Uni.

347 Ekwue, E.I., Stone, R.J., & Bhagwat, D. (2006). Thermal Conductivity of Some Compacted
348 Trinidadian Soils as affected by Peat Content. *Biosystems Engineering*, 94, 461–469.

349 Eslami, H., Rosin-Paumier, S., Abdallah, A., & Masrouri, F. (2014). Impact of temperature
350 variation on penetration test parameters in compacted soils. *European Journal of*
351 *Environmental and Civil Engineering*. doi: 10.1080/19648189.2014.960952.

352 Farouki, O.T. (1981). Thermal properties of soils. Monograph 81-1. *U.S. Army Cold Regions*
353 *Research and Engineering Laboratory*, Hanover, New Hampshire, USA.

354 Fleureau, J.M, & Indarto. (1993). Comportement du limon de Jossigny remanié soumis à une
355 pression interstitielle négative. *Revue française de géotechnique*, 62, 59–66.

356 Giordano, N., Comina, C., Mandrone, G., & Cagni, A. (2016). Borehole thermal energy
357 storage (BTES). First results from the injection phase of a living lab in Torino (NW Italy).
358 *Renewable Energy*, 86, 993–1008.

359 Hanna, M.A., Chikhani, A.Y., & Salama, M.M.A. (1993). Thermal analysis of power cables
360 in multi-layered soil. Part 1: Theoretical model. *IEEE Transactions on Power Delivery*, 8(3),
361 761–771.

362 Hiraiwa, Y., & Kasubuchi, T. (2000). Temperature dependence of thermal conductivity of soil
363 over a wide range of temperature (5-75°C). *European Journal of Soil Science*, 51(2), 211–
364 218.

365 Johansen, O. (1977). Thermal conductivity of soils. *U.S. Army Cold Regions Research and*
366 *Engineering Laboratory*, Hanover, New Hampshire, USA.

367 Kersten, M.S. (1949). *Thermal properties of soils* (Report No. 28). University of Minnesota:
368 Retrieved from the University of Minnesota Digital Conservancy,
369 <http://purl.umn.edu/124271>.

370 De Lieto Vollaro, R., Fontana, L., & Vallati, A. (2011). Thermal analysis of underground
371 electrical power cables buried in non-homogeneous soils. *Applied Thermal Engineering*,
372 31(5), pp.772–778.

373 Navarro, L., De Gracia, A., Niall, D., Castell, A., Browne, M., McCormack, S.J.,... Cabeza,
374 L.F. (2016). Thermal energy storage in building integrated thermal systems: A review. Part 2.
375 Integration as passive system. *Renewable Energy*, 85, 1334–1356.

376 Pahud, D. (2002). Geothermal energy and heat storage. *SUPSI – DCT – LEEE Laboratorio di*
377 *Energia, Ecologia ed Economia*.

378 Péron, H., Knellwolf, C., & Laloui, L. (2011). A method for the geotechnical design of heat
379 exchanger piles. In H. Jie & D. E. Alzamora (Eds.), *Geo-Frontiers 2011: Advances in*
380 *Geotechnical Engineering* (470–479). Dallas, TX: American Society of Civil Engineers.
381 Geotechnical Special Publications 211.

382 Rutqvist, J., Wu, Y.-S., Tsang, C.-F., & Bodvarsson, G. (2002). A modeling approach for
383 analysis of coupled multiphase fluid flow, heat transfer, and deformation in fractured porous
384 rock. *International Journal of Rock Mechanics and Mining Sciences*, 39(4), 429–442.

385 Smits, K., Sakaki, T., Howington, S., Peters, J., & Illangasekare, T. (2013). Temperature
386 dependence of thermal properties of sands across a wide range of temperatures (30-70°C).
387 *Vadose Zone Journal*, 12 : doi 10.2136/vzj2012.0033.

388 Standard ASTM (2000). D5334 – 14: Standard test method for determination of thermal
389 conductivity of soil and soft rock by thermal needle probe procedure (8p). West
390 Conshohocken, PA www. ASTM. org: ASTM International.

391 Tang, A. (2005). *Effet de la température sur le comportement des barrières de confinement*.
392 (PhD thesis). École Nationale des Ponts et Chaussées, Paris, France. Retrieved from
393 <http://pastel.archives-ouvertes.fr/pastel-00001594/>

394 Zhang, T., Cai, G., Liu, S., & Puppala, A. J. (2017). Investigation on thermal characteristics
395 and prediction models of soils. *International Journal of Heat and Mass Transfer*, 106, 1074-
396 1086.

397 Zhao, D., Qian, X., Gu, X., Jajja, S.A. & Yang, R. (2016). Measurement Techniques for
398 Thermal Conductivity and Interfacial Thermal Conductance of Bulk and Thin Film Materials.
399 *Journal of Electronic Packaging*, 138(4), 040802, 64p.

400 *Table 1. Mineralogical composition of the raw materials*

Material	Ref.	Quartz	calcium carbonate	Feldspar	clay minerals	Others
Illitic soil	I	Traces	12% Calcite	Traces	77% Illite 10% Kaolinite	
Plaisir Loam	PL	81%	5% Calcite 7% Dolomite	3%	5%	
Jossigny Loam	JL	98%	Traces	1%	1%	
Xeuilley Loam	XL	83%	2%	3%	11%	1% Goethite
Hostun Sand	S	97.4%	Traces			2.6%

401

402

403

404 *Table 2. The characteristics of the studied materials*

Properties	Illitic soil I	Plaisir loam PL	Jossigny loam JL Fleureau & Inderto (1993)	Xeuilley loam XL Blanck et al. (2011)
Grain size distribution				
Passer - by 80 μm	100	41	80	95
Passer - by 2 μm	85	20	28	25
Atterberg limits				
Plastic limit (%)	34	20.6	16 - 19	28
Liquid limit (%)	65	27.3	37	37
Plasticity index	31	6.7	18 - 21	9
Specific surface				
MBV(g/100g)	5.41	1.85	-	3.1
Carbonate content				
CaCO ₃	-	0.8	-	1.3
Proctor compaction				
WOPN (%)	31.3	16	15.5	18.5
$\gamma_{\text{dmax}}/\gamma_{\text{w}}$	1.43	1.81	1.75	1.71
$\gamma_{\text{max}}/\gamma_{\text{w}}$	1.88	2.10	2.02	2.03
Soil Class				
GTR Classification	A3	A1	A2	A2
USCS Classification	MH	CL	CL	ML

405

406

407

408

409

410

411

412 *Table 3. Composition and parameters of the standard Proctor curve for the mixtures*

Mixture	Composition	WOPN (%)	ρ_{dmax} (Mg/m ³)	ρ_{hOPN} (Mg/m ³)
S+I	50% Hostun sand and 50% Illitic soil	18.6	1.71	2.03
S+JL	50% Hostun sand and 50% Jossigny Loam	13.6	1.89	2.15
S+XL	50% Hostun sand and 50% Xeuilley Loam	13.7	1.88	2.14

413

414

415

416

417

418 *Table 4. Performed tests as a function of material type*

Series	Variables	Materials				
		I	S+I	PL	S+JL	S+XL
1	γ	+	+			
2	w	+	+			
3	mineralogy and particle size	+	+	+		
4	w and γ	+	+	+	+	+
5	w and γ and T	+	+	+		
6	w and γ and T (cycle)			+		

419

420

421 *Table 5. Range and precision of sensors SH-1 and TR-1*

Sensor	Propriety	Measure range	Precision
TR-1	Thermal conductivity (W.m ⁻¹ .K ⁻¹)	0.1 - 0.2	± 0.02
		0.2 - 4	± 10 %
SH-1	Thermal conductivity (W.m ⁻¹ .K ⁻¹)	0.02 - 0.2	± 0.01
		0.2 - 2	± 10 %
SH-1	Thermal diffusivity (mm ² /s)	0.1 - 1	± 10 %
SH-1	Volumetric heat capacity (MJ.m ⁻³ K ⁻¹)	0.5 - 4	± 10 %

422

423

424

425

426

427

428 *Table 4. Temperature programme applied on PL (6th series)*

Program	Stage 1		Stage 2		NB cycle
	T°C	Time	T°C	Time	
P1	20	9h	50	9h	60
P2	20	2h	50	4h	60
P3	20	9h	50	9h	4

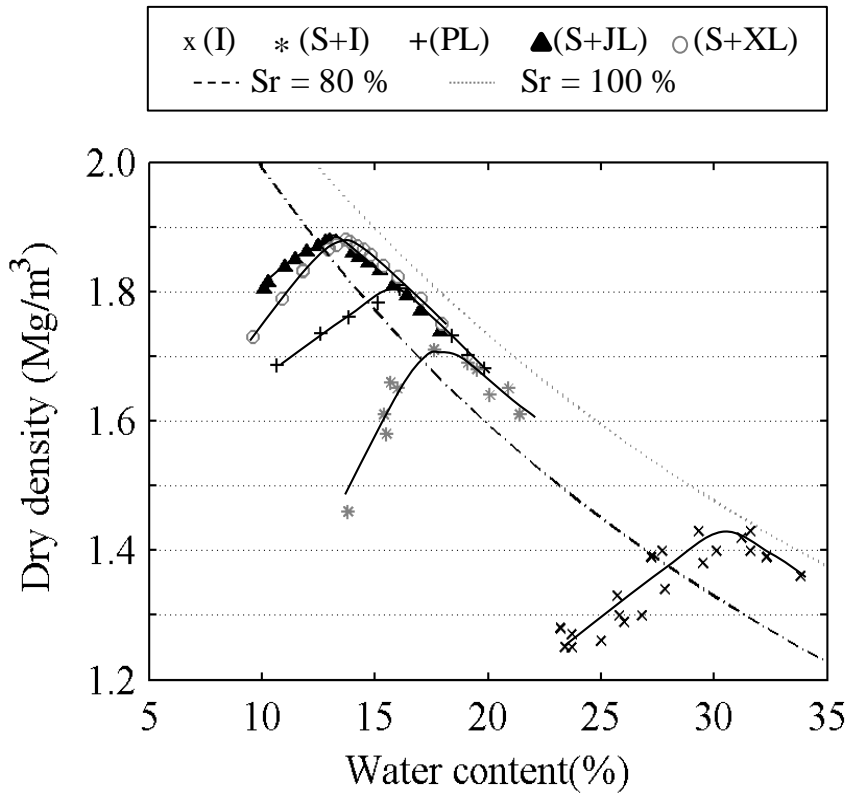
429

430

431

432

433



434

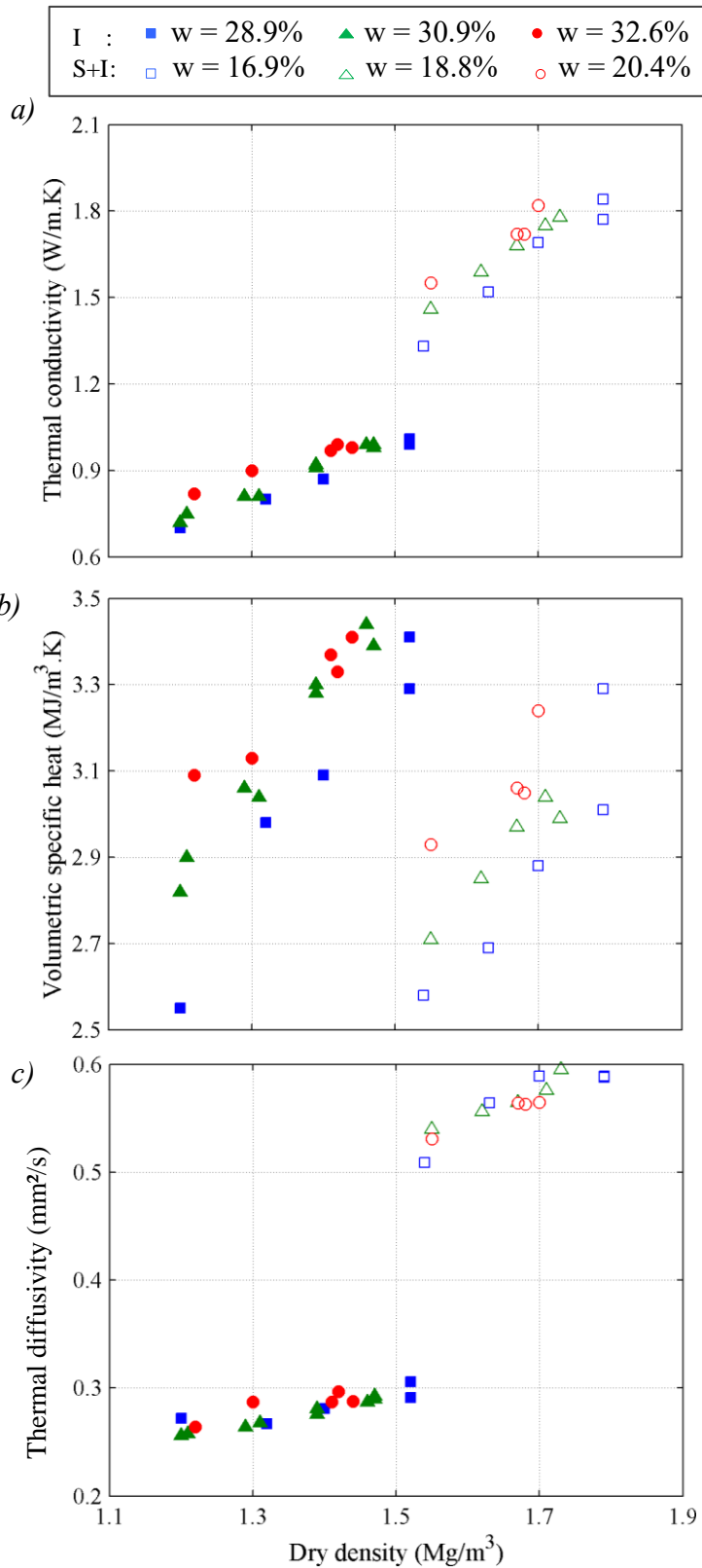
435 *Figure 1. Compaction curves of the studied materials.*

436

437

438

439

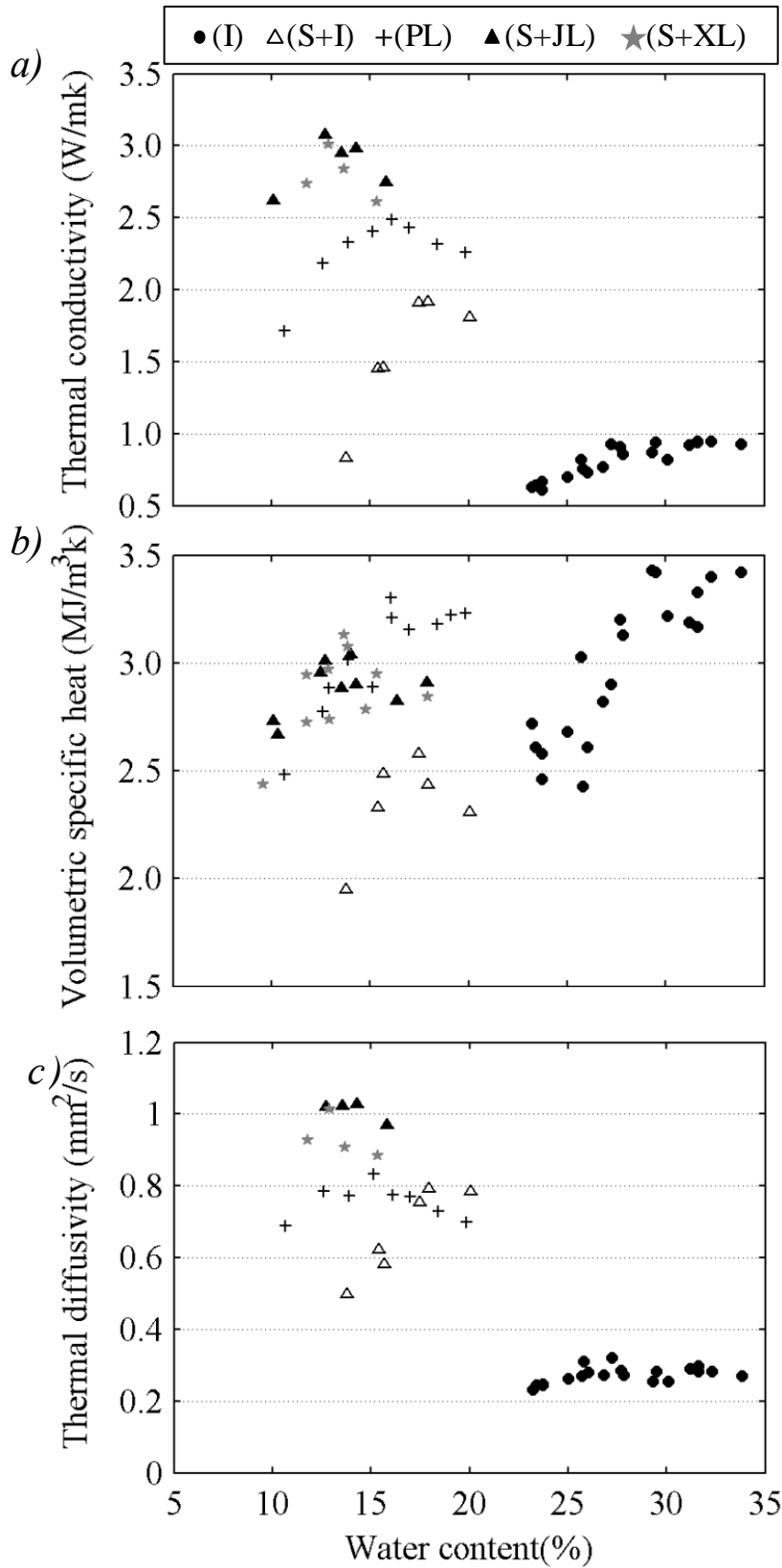


440

441 *Figure 2. Evolution of the (a) Thermal conductivity, (b) Volumetric heat capacity and (c)*

442 *Thermal diffusivity as a function of dry density at different water contents for the illitic*

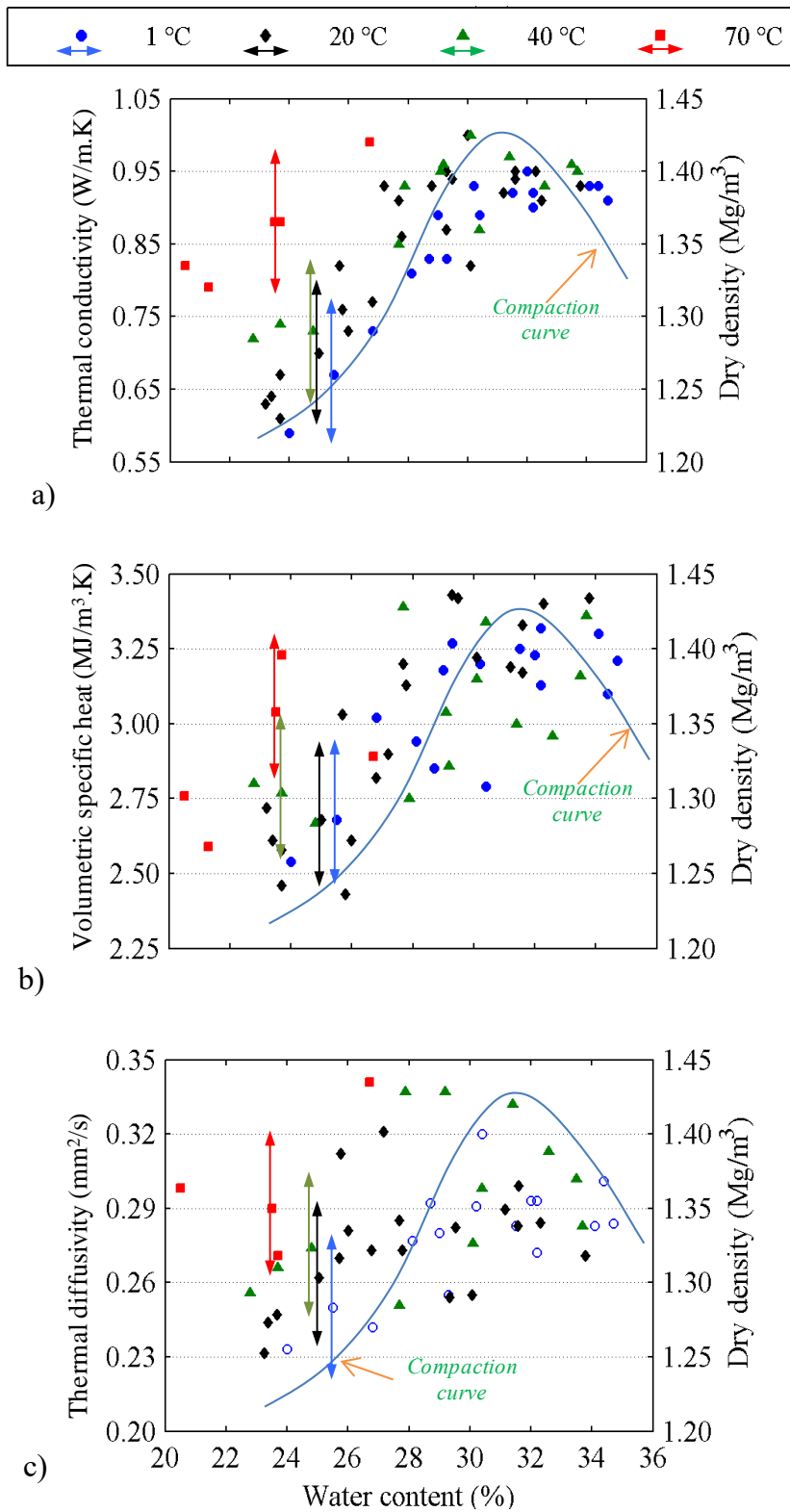
443 *material (I) and the sand-illitic material mixture (S+I) (1st and 2nd series).*



444

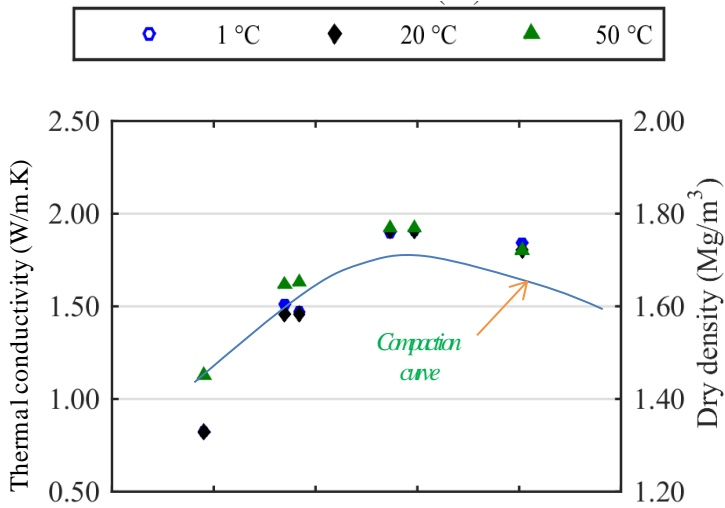
445 *Figure 3. (a) Thermal conductivity, (b) Volumetric heat capacity and (c) thermal diffusivity as*

446 *a function of water content and dry density of materials (4th series).*

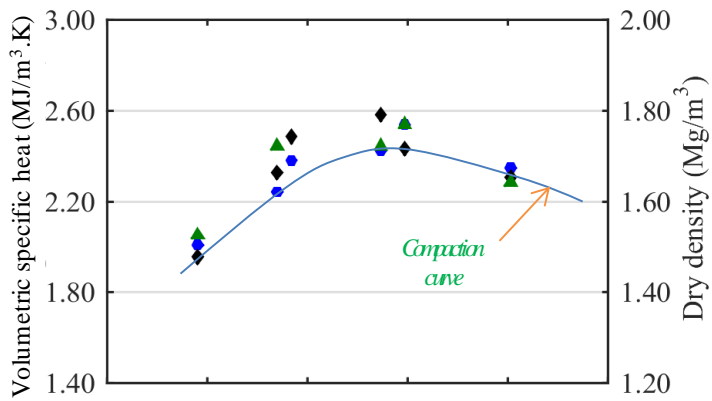


447
448

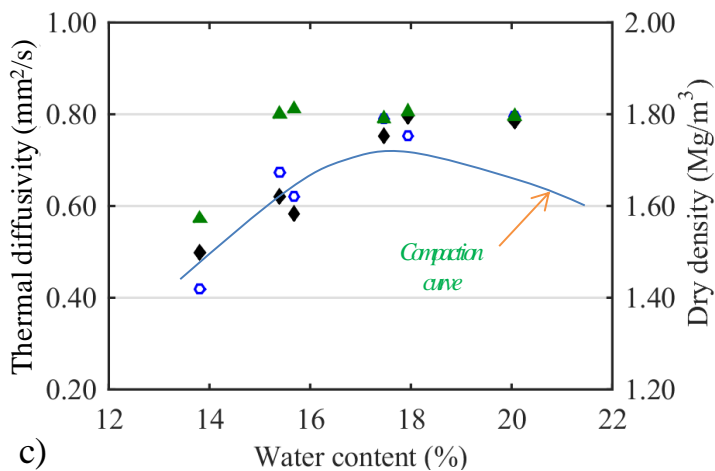
449 *Figure 4. Evolution of the thermal properties of the illitic soil (I) according to the*
450 *temperature and uncertainty (double arrow) : (a) Thermal conductivity, (b) Volumetric heat*
451 *capacity and (c) Thermal diffusivity (5th series).*



a)



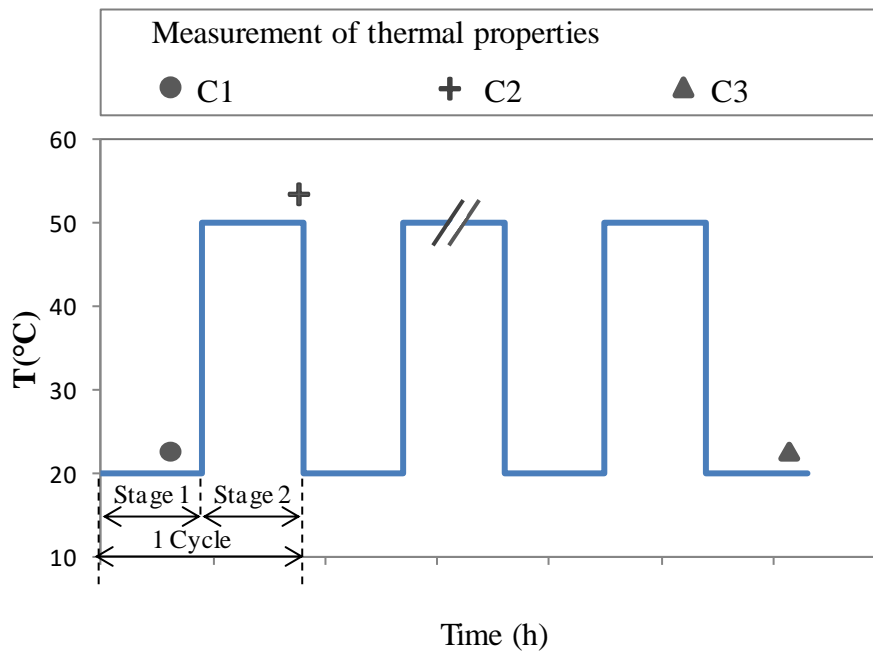
b)



c)

452
 453 *Figure 5. Evolution of the thermal properties of the sand-illitic soil mixture (S+I) according*
 454 *to the temperature: (a) Thermal conductivity, (b) Volumetric heat capacity and (c) Thermal*
 455 *diffusivity (5th series).*

456



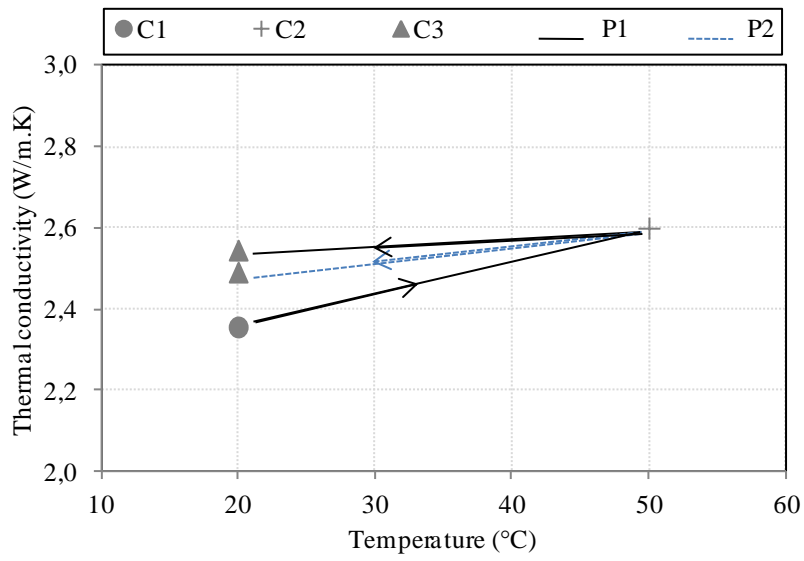
457

458 *Figure 6. The chronology of measurements as a function of cyclic temperature variation*

459 *applied to the PL samples (6th series).*

460

461

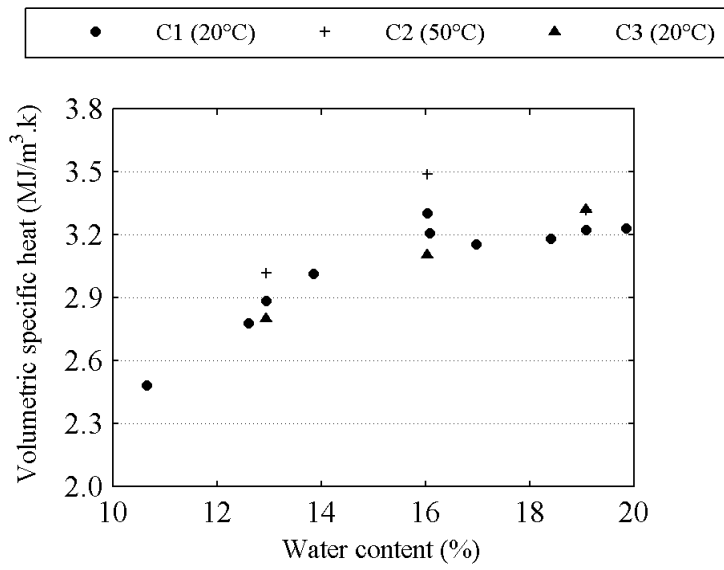


462

463 *Figure 7. Warming effect on thermal conductivity of PL (P1, P2, 6th series).*

464

465



466

467 *Figure 8. Warming effect on volumetric heat capacity of PL (P3, 6th series).*